ISSN 1063-7826, Semiconductors, 2016, Vol. 50, No. 7, pp. 869–875. © Pleiades Publishing, Ltd., 2016.
Original Russian Text © A.A. Kudryashov, V.G. Kytin, R.A. Lunin, V.A. Kulbachinskii, A. Banerjee, 2016, published in Fizika i Tekhnika Poluprovodnikov, 2016, Vol. 50, No. 7, pp. 886–892.

ELECTRONIC PROPERTIES OF SEMICONDUCTORS

Effect of Thallium Doping on the Mobility of Electrons in Bi_2Se_3 and Holes in Sb_2Te_3

A. A. Kudryashov[a], V. G. Kytin[a], R. A. Lunin[a], V. A. Kulbachinskii[a, b]*, and A. Banerjee[c]

[a] *Faculty of Physics, Moscow State University, Moscow, 119991 Russia*
[b] *National Research Nuclear University "MEPhI", Kashirskoe sh. 31, Moscow, 115409 Russia*
[c] *Department of Physics, University of Calcutta, 92 A P C Road, Kolkata 700009, India*
* *e-mail: kulb@mig.phys.msu.ru*

Submitted December 10, 2015; accepted for publication December 17, 2015

Abstract—The Shubnikov–de Haas effect and the Hall effect in n-$Bi_{2-x}Tl_xSe_3$ ($x = 0$, 0.01, 0.02, 0.04) and p-$Sb_{2-x}Tl_xTe_3$ ($x = 0$, 0.005, 0.015, 0.05) single crystals are studied. The carrier mobilities and their changes upon Tl doping are calculated by the Fourier spectra of oscillations. It is found shown that Tl doping decreases the electron concentration in n-$Bi_{2-x}Tl_xSe_3$ and increases the electron mobility. In p-$Sb_{2-x}Tl_xTe_3$, both the hole concentration and mobility decrease upon Tl doping. The change in the crystal defect concentration, which leads to these effects, is discussed.

DOI: 10.1134/S1063782616070113

1. INTRODUCTION

The use of thermoelectric devices allows direct thermal-to-electric energy conversion. In this case, thermal generators can use this thermal energy which is usually released to the ambient atmosphere. This is extremely important in the world today in the context of limited power resources [1, 2]. A good thermoelectric material should have a high conductivity σ to minimize losses to heating, a low thermal conductivity k, and a high Seebeck coefficient S, i.e., high thermoelectric efficiency $Z = S^2\sigma/k$ [3]. To obtain materials with high Z, the effect of various factors, including doping, on the above parameters should be studied [4].

Bismuth selenide (Bi_2Se_3) and $Bi_2Te_{3-x}Se_x$ alloys, including the most compensated Bi_2Te_2Se compound, are well studied [5]. The relation of the thermoelectric properties to the $Bi_2Te_{3-x}Se_x$ composition is traced in [6]. An important parameter of thermoelectrics is the electron or hole mobility. The carrier mobility depends on the scattering mechanisms and, in bismuth–antimony tellurides and selenides, it also depends on doping. The carrier mobility usually decreases with increasing dopant concentration [7, 8]. However, sometimes, the carrier mobility increases under low doping; e.g., such an effect in bismuth telluride was observed upon doping with germanium or indium [9].

Antimony telluride (Sb_2Te_3) is a known thermoelectric p-type material [10–12]. A similar but n-type material is bismuth selenide (Bi_2Se_3) which is used in thermoelectric devices and has high Z at room temperature [13–17]. These materials are narrow-gap semiconductors of rhombohedral structure with $R\bar{3}m$–D_{3d}^5 symmetry. The layered structure leads to a low thermal conductivity and high thermoelectric efficiency Z. In Sb_2Te_3, a large number of charged antisite defects (Sb atoms occupy Te sites in the lattice) are usually observed, which leads to p-type conductivity [10]. In addition to other defects, such as Te vacancies, they are scattering centers and affect the thermoelectric power S [11, 18].

Despite extensive studies of both bismuth and antimony tellurides and selenides, there are only a few papers on the effect of Tl doping on the properties of Bi_2Se_3 [19], Sb_2Te_3 [20], and $Sb_{1.5}Bi_{0.5}Te_3$ [21].

In this work, we study the effect of the thallium doping of p-Sb_2Te_3 and n-Bi_2Se_3 single crystals on the Hall carrier mobilities and mobilities obtained from the Shubnikov–de Haas (ShdH) effect in magnetic fields of 30–38 T.

2. EXPERIMENTAL

Thallium-doped p-$Sb_{2-x}Tl_xTe_3$ ($x = 0$, 0.005, 0.015, 0.05) and n-$Bi_{2-x}Tl_xSe_3$ ($x = 0$, 0.01, 0.02, 0.04) single crystals grown by the Bridgman method were studied. In measurements of the Shubnikov–de Haas effect, the current was directed along the $\mathbf{C}_2$ axis in the basal plane, the magnetic field was perpendicular to the basal plane along the $\mathbf{C}_3$ axis. The Shubnikov–de Haas effect was measured in pulsed magnetic fields at a temperature of $T = 4.2$ K [22]. The thallium con-

Table 1. Electron concentration n, Fermi energy E_F, quantum mobility μ_q, determined from the Shubnikov–de Haas effect, and Hall mobility μ_H of n-$Bi_{2-x}Tl_xSe_3$ samples

Sample no.	Composition	n, 10^{19} cm^{-3}	E_F, meV	μ_q, cm^2/(V s)	μ_H, cm^2/(V s)
1	Bi_2Se_3	2.2	161.7	340	1030
2	$Bi_{1.99}Tl_{0.01}Se_3$	2.1	160.1	520	1370
3	$Bi_{1.98}Tl_{0.02}Se_3$	1.9	153.4	360	1374
4	$Bi_{1.96}Tl_{0.04}Se_3$	1.6	140.3	930	1510

Table 2. Light-hole concentration p, Fermi energy E_F, and quantum mobility μ_q of p-$Sb_{2-x}Tl_xTe_3$ samples, determined from the Shubnikov–de Haas effect

Sample no.	Composition	p, 10^{19} cm^{-3}	E_F, meV	μ_q, cm^2/(V s)
1	Sb_2Te_3	2.8	97.1	1160
2	$Sb_{1.995}Tl_{0.005}Te_3$	2.7	93.7	790
3	$Sb_{1.985}Tl_{0.015}Te_3$	2.6	92.2	760
4	$Sb_{1.95}Tl_{0.05}Te_3$	1.4	61.1	420

centration is given according to loading during single-crystal growth. The carrier concentrations and Fermi energies were determined from the ShdH-effect data by the technique described in [22–25]. Some parameters of the samples under study are given in Table 1 for n-$Bi_{2-x}Tl_xSe_3$ and in Table 2 for p-$Sb_{2-x}Tl_xTe_3$. The procedure for calculating the quantum mobilities μ_q is given in the next section.

We can see in Tables 1 and 2 that the electron concentration decreases in n-Bi_2Se_3; the hole concentration also decreases in thallium-doped p-Sb_2Te_3.

3. MEASUREMENT RESULTS AND DISCUSSION

For the $Bi_{2-x}Tl_xSe_3$ ($x = 0.01, 0.02, 0.04$) samples, the Shubnikov–de Haas effect in strong magnetic fields was also studied at magnetic field **B** orientation along the $\mathbf{C}_3$ axis. Figure 1 shows the SdH oscillations and the Hall effect for the samples under study; Fig. 2 shows the Fourier spectra of oscillations. In all samples, only one frequency was observed, which corresponds to one ellipsoid of the electron Fermi surface of light electrons in Bi_2Se_3. Experimental data on the Shubnikov–de Haas effect are used to calculate the electron concentration and the Fermi energy which are given in Table 1. The calculation procedure is described in [22–25]. The electron concentration and Fermi energy in Bi_2Se_3 decrease upon Tl doping.

For $Sb_{2-x}Tl_xTe_3$ single crystals, the Shubnikov–de Haas oscillations were measured (see Fig. 3). As noted above, all measurements were performed for magnetic field orientation along the $\mathbf{C}_3$ axis. In this case, for the six-ellipsoid Fermi surface of light holes, all ellipsoid sections coincide and only one oscillation frequency f is observed, which is seen in the Fourier transform shown in the inset in Fig. 3. The oscillation frequency decreases with increasing doping, which corresponds to a decrease in the light-hole concentration. The oscillation frequencies, light-hole densities, and Fermi energies in the samples under study were determined from Fourier analysis (see Table 2).

The data obtained from the Shubnikov–de Haas effect can be used to calculate the carrier mobilities and their changes upon doping of the studied $Bi_{2-x}Tl_xSe_3$ and $Sb_{2-x}Tl_xTe_3$ alloys. When determining the carrier mobilities, the transport and quantum relaxation times should be distinguished [26–30]. The transport relaxation time τ_t of the electron momentum is controlled by the average time between events of elastic scattering at impurities, which significantly change the momentum direction, and can be written as

$$\frac{1}{\tau_t} = \int_0^\pi \sigma(\varphi)(1-\cos\varphi)d\varphi, \quad (1)$$

where $\sigma(\varphi)$ is proportional to the scattering probability per unit time at angle φ. The quantum lifetime τ_q (single-particle relaxation time) is derived by averaging the time between arbitrary scattering events and is given by the expression

$$\frac{1}{\tau_q} = \int_0^\pi \sigma(\varphi)d\varphi. \quad (2)$$

Due to the factor $(1 - \cos\varphi)$ in the expression for τ_t, the transport scattering time can differ from the quantum one. For isotropic scattering, e.g., at phonons, these scattering times are equal. However, for Coulomb scattering at ionized impurities, $\sigma(\varphi)$ is high for scattering at small angles; therefore, τ_t can be several times higher than τ_q.

An analysis of the dependences of the Shubnikov–de Haas oscillation amplitude on the magnetic field makes it possible to determine the quantum electron mobilities $\mu_q = (e/m)\tau_q$ [26]. The envelope of the Shubnikov–de-Haas-oscillation magnetoresistance exponentially depends on the quantum mobility as [27, 31–34]

$$\Delta\rho_{xx} = A\sum_{s=1}^{\infty}\exp\left(-\frac{\pi s}{\mu_q B}\right) \times\cos\left[\frac{2\pi s E_F}{\hbar\omega_c} - s\pi\right]\frac{2\pi^2 s k_B T/\hbar\omega_c}{\sinh(2\pi^2 s k_B T/\hbar\omega_c)}, \quad (3)$$

where T is the temperature, k_B is the Boltzmann constant, and ω_c is the cyclotron frequency.

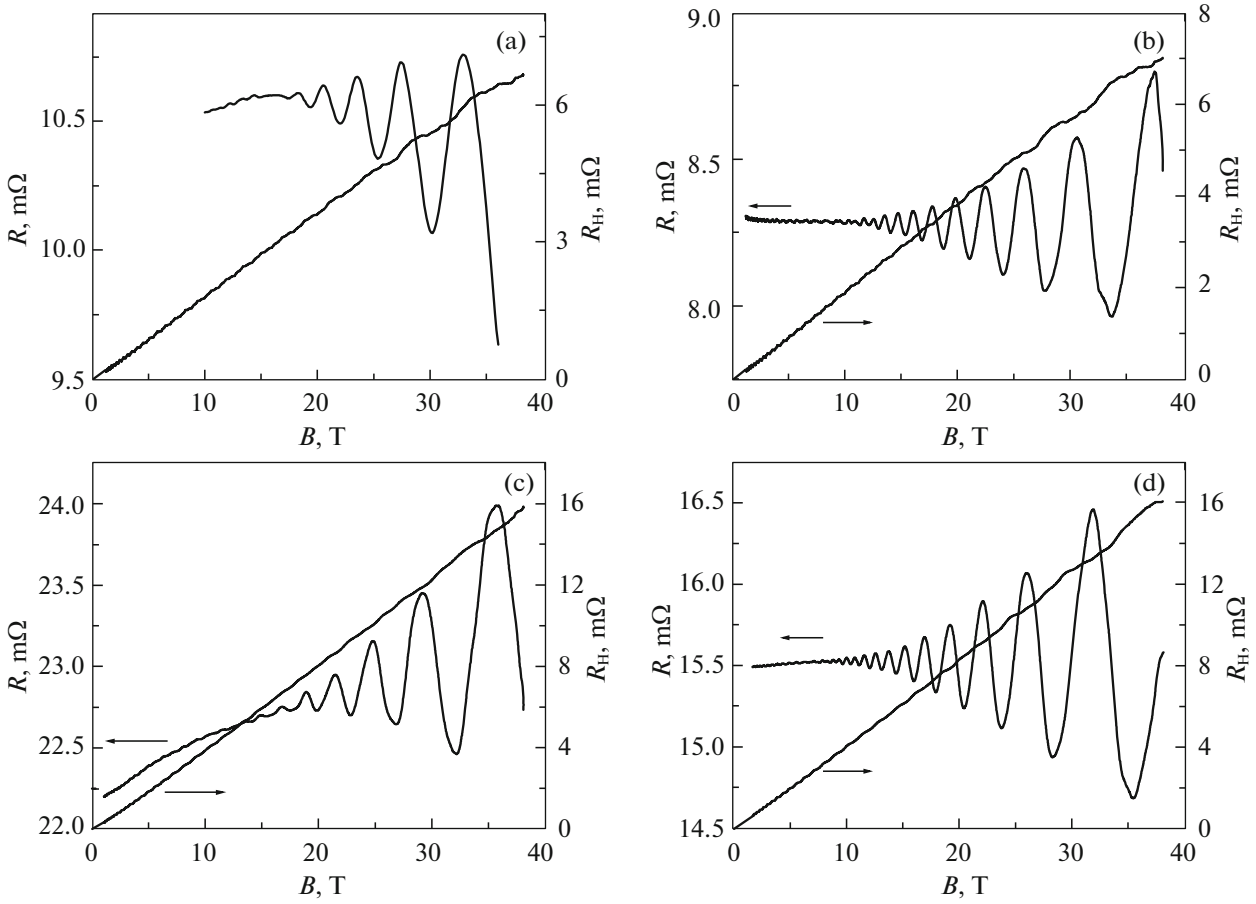

Fig. 1. Magnetoresistance R and Hall resistance R_H at a temperature of 4.2 K of (a) Bi_2Se_3, (b) $Bi_{1.99}Tl_{0.01}Se_3$, (c) $Bi_{1.98}Tl_{0.02}Se_3$, and (d) $Bi_{1.96}Tl_{0.04}Se_3$ samples.

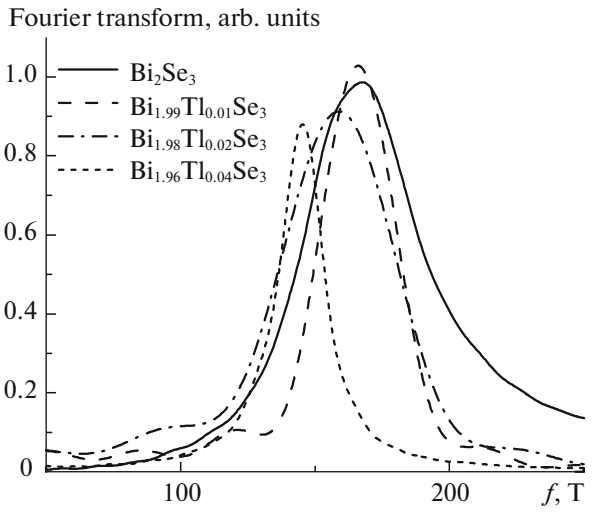

Fig. 2. Fourier spectra of Shubnikov–de Haas oscillations for the $Bi_{2-x}Tl_xSe_3$ samples.

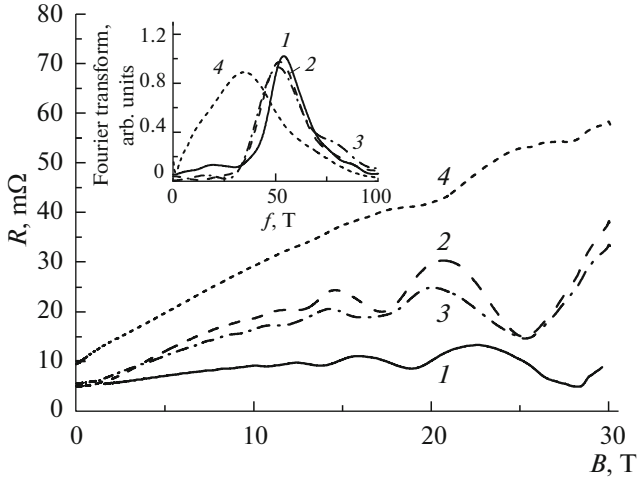

Fig. 3. SdH oscillations at a temperature of 4.2 K for the $Sb_{2-x}Tl_xTe_3$ samples, x = (*1*) 0, (*2*) 0.005, (*3*) 0.015, and (*4*) 0.05. The inset shows the Fourier spectra of corresponding oscillations.

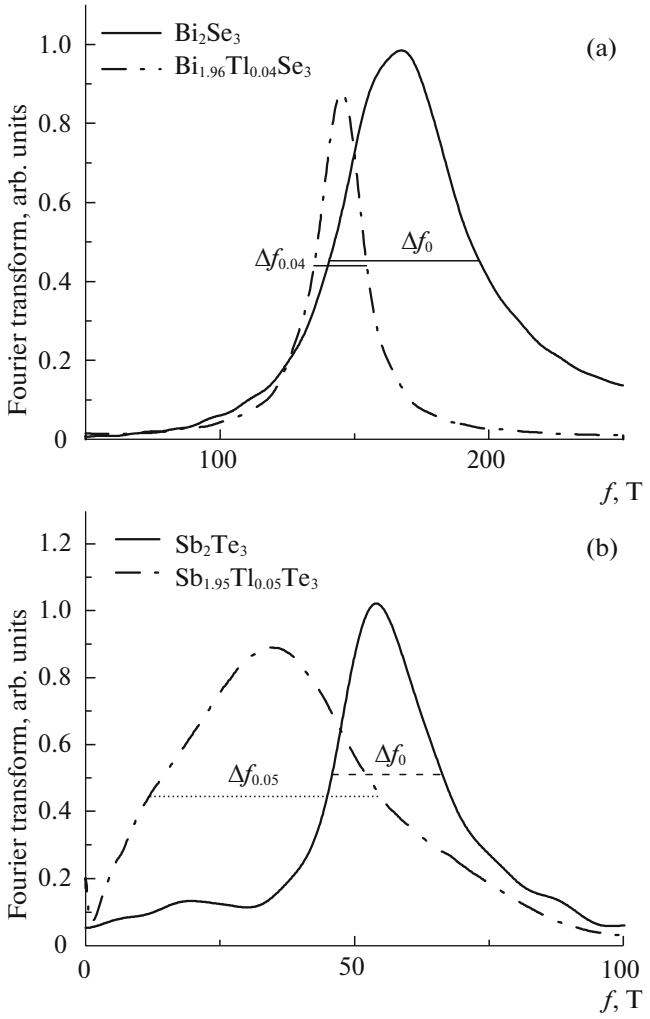

Fig. 4. Fourier spectra of SdH oscillations for various samples: (a) Bi_2Se_3 and $Bi_{1.96}Tl_{0.04}Se_3$; the corresponding peak widths Δf_0 and $\Delta f_{0.04}$ are shown; (b) Sb_2Te_3 and $Sb_{1.95}Tl_{0.05}Te_3$, the corresponding peak widths $\Delta f_{0.05}$ and Δf_0 are shown.

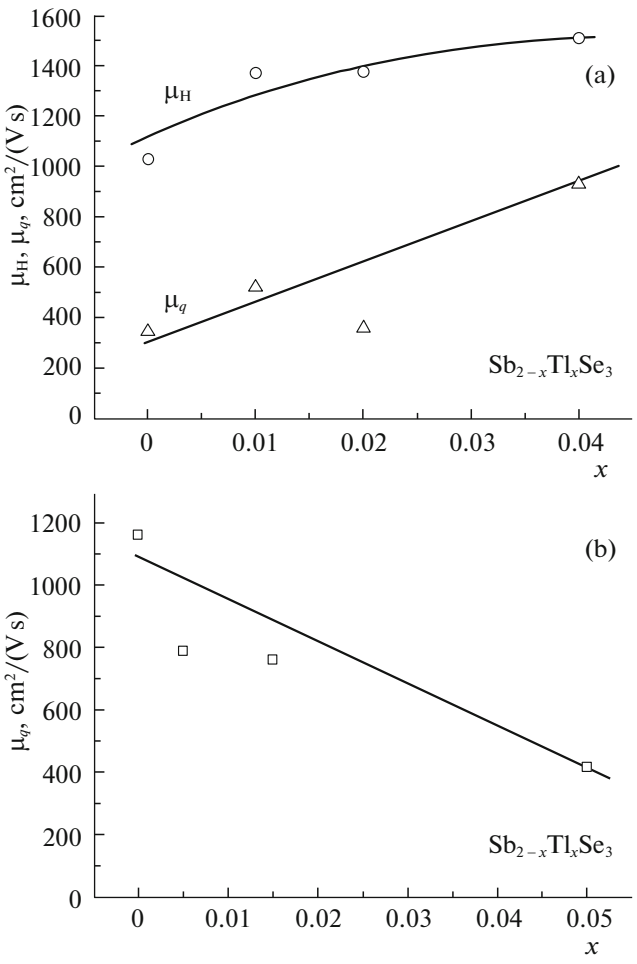

Fig. 5. (a) Electron Hall mobility μ_H and quantum mobility μ_q as functions of the thallium concentration x for the $Bi_{2-x}Tl_xSe_3$ samples, and (b) the quantum hole mobility μ_q as a function of the thallium concentration x for $Sb_{2-x}Tl_xTe_3$ samples.

The simplest method for determining the quantum mobility was proposed in [35], where it was shown that the Fourier spectrum of the first harmonic of the Shubnikov–de Haas oscillations follows the expression

$$A(f) \propto \frac{1}{[1/4\mu_q^2 + (f - f_0)^2]^{1/2}}, \quad (4)$$

where μ_q is the quantum mobility, f is the frequency, and f_0 is the frequency of the Fourier-spectrum maximum. It follows from formula (4) that the Fourier-peak width Δf (full-width at half-maximum) can be used to determine the quantum mobility [35],

$$\mu_q = \frac{\sqrt{3}}{\Delta f}. \quad (5)$$

The Fourier-peak widths Δf for the Bi_2Se_3 and $Bi_{1.96}Tl_{0.04}Se_3$ samples are shown in Figs. 4a (Δf_0 and $\Delta f_{0.04}$, respectively); for Sb_2Te_3, $Sb_{1.95}Tl_{0.05}Te_3$ samples (Δf_0 and $\Delta f_{0.05}$, respectively), they are shown in Fig. 4b. The dependences of the quantum carrier mobilities on the thallium concentration x, determined by formula (5), are shown in Fig. 5 for the $Bi_{2-x}Tl_xSe_3$ and $Sb_{2-x}Tl_xTe_3$ samples. Furthermore, Fig. 5a shows the electron Hall mobilities for $Bi_{2-x}Tl_xSe_3$.

Formula (4) was derived in the approximation of a measurement temperature much lower than the Dingle temperature $T_D = (e\hbar/2\pi k_B)(1/m_c^*\mu_q)$; therefore, the last factor in formula (3), containing temperature, is 1/2. For the samples under study, this condition is satisfied, since the measuring temperature is 4.2 K; at the cyclotron electron mass for n-$Bi_{2-x}Tl_xSe_3$ in the lower band $m_c^* = 0.105\ m_0$ [36], the Dingle tempera-

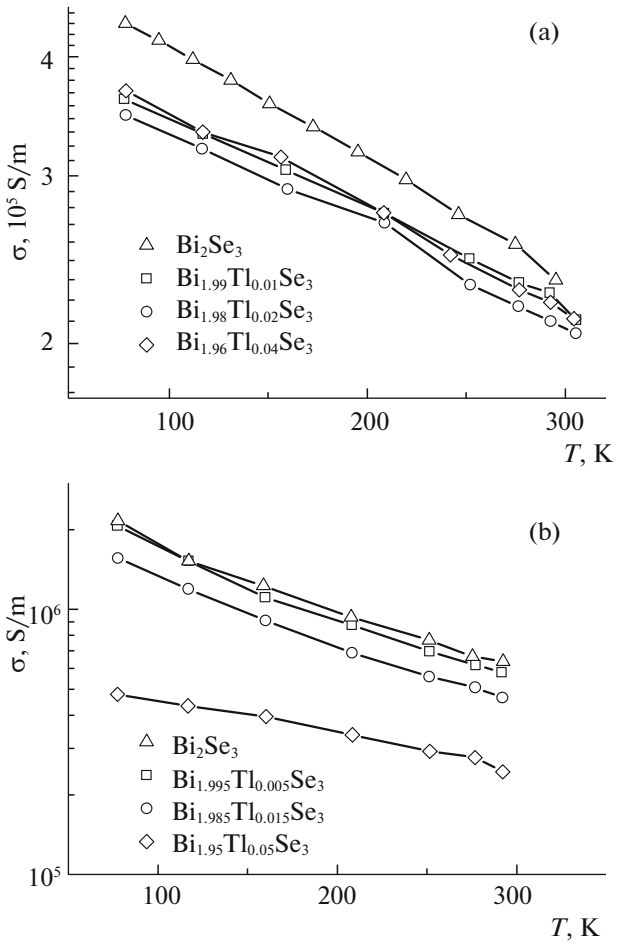

Fig. 6. Temperature dependences of the conductivity (on the log scale) for (a) $Bi_{2-x}Tl_xSe_3$ and (b) $Sb_{2-x}Tl_xTe_3$ samples.

ture is from 22 to 60 K for samples with different thallium contents. For p-$Sb_{2-x}Tl_xTe_3$, the cyclotron mass of light holes in the upper band is $m_c^* = 0.083m_0$ [37], and the Dingle temperature is 23–62 K for different thallium concentrations.

Figure 5a also shows the electron Hall mobilities for the $Bi_{2-x}Tl_xSe_3$ samples. These samples contain only one group of carriers; therefore, the Hall mobility is equal to the transport mobility $\mu_t = (e/m^*)\tau_t$. The ratio of the transport mobility to the quantum mobility is 3 for Bi_2Se_3, which, according to formulas (1) and (2), indicates small-angle electron scattering in this material. As the thallium concentration increases to $x = 0.04$, this ratio decreases to 1.6; this means that the nature of electron scattering in $Bi_{1.96}Tl_{0.04}Se_3$ changes and scattering becomes more isotropic. In the $Sb_{2-x}Tl_xTe_3$ samples, there are two occupied hole bands [10, 37]; therefore, the Hall mobility is not equal to the transport mobilities in each band.

As seen in Table 1 and Fig. 6a, the $Bi_{2-x}Tl_xSe_3$ conductivity changes insignificantly upon Tl doping, while the Fermi energy (electron concentration) significantly decreases. This indicates an increase in the electron mobility.

Qualitatively, this can be understood when considering the probability of forming charged point defects in this material and changes in their concentration upon thallium doping. If Bi_2Se_3 is grown under stoichiometric conditions, a bismuth excess is formed [38]. In this case, antisite defects, i.e., negatively and positively charged bismuth atoms are formed at selenium sites, Bi_{Se}^{-1}, and positively charged vacancies in the selenium sublattice, V_{Se}^{+2} [39], are formed. The vacancy concentration is higher and the $Bi_{2+\delta}Se_3$ crystals are n-type. Thallium atoms substitute Bi at lattice sites, forming Tl_{Bi} defects. Thallium can form uncharged neutral Tl_{Bi}^{x} defects with a valence of +3. In this case, no free carriers are formed. From the chemical viewpoint, the state with +1 valence is more stable, i.e., Tl can capture two electrons from the conduction band and lower the electron concentration. The nonlinear dependences of the electron concentration on the Tl content [3] suggest that it is not a single process. In thallium-doped crystals, the concentration of charged Se vacancies can change, which also lowers the electron concentration [19].

For $Bi_{2-x}Tl_xSe_3$, the electron-scattering parameter r changes insignificantly upon thallium doping [24, 25]. An increase in the electron mobility and a minor change in r suggest that the number of charged point defects decreases upon thallium doping. This is also indicated by a decrease in the ratio of the transport-to-quantum mobility from 3 to 1.6 upon thallium doping. Thus, the decrease in charged point defects V_{Se}^{+2} prevails over Tl_{Bi}^{-2} defect formation.

In undoped Sb_2Te_3 samples, the carrier-scattering parameter r is close to $-1/2$, which indicates preferential scattering at acoustic phonons [24, 25]. Thallium doping results in an increase in r, which indicates a change in the scattering nature in favor of scattering at ionized impurities [24, 25]. In $Sb_{2-x}Tl_xTe_3$, the effect of thallium doping on the above changes in the nature of scattering is consistent with the conductivity change upon doping, shown in Fig. 6b (see Table 2). Conductivity decreases significantly faster than the Fermi energy (hole concentration). This is possible only if the hole mobility decreases upon thallium doping. The temperature dependence of the conductivity becomes weaker, i.e., the contribution of scattering at ionized impurities is added to the scattering.

Upon doping, thallium atoms substitute antimony in the Sb_2Te_3 crystal. Since they do not have a sufficient number of electrons at the p level to form a σ bond, they donate two 6s electrons to the p orbital,

and the *s* orbital remains unoccupied. Thus, the substitution of antimony with thallium results in the formation of uncharged Tl^{x}_{Sb} defects. The formed Tl^{x}_{Sb} defects do not contribute to the hole concentration; however, since thallium has a lower electronegativity in comparison with antimony, the bond between defects and tellurium atoms, Tl^{x}_{Sb}–Te, is more polar, than the Sb–Te bond. In other words, a positive charge arises in $Tl^{(1+\sigma)}_{Sb}$ point defects, which increases the bond-ionization ratio. At these positive charges, additional scattering does arise, which increases the scattering parameter *r*. The more polar bond results in suppression of the formation of Sb^{1}_{Te} antisite defects (responsible for the high initial hole concentration) which appear under conditions of an almost completely unpolarized bond in the lattice [20].

4. CONCLUSIONS

The Shubnikov–de Haas effect and the Hall effect in n-$Bi_{2-x}Tl_xSe_3$ ($x = 0$, 0.01, 0.02, 0.04) and p-$Sb_{2-x}Tl_xTe_3$ ($x = 0$, 0.005, 0.015, 0.05) single crystals were studied. It was shown that thallium doping decreases the concentration of electrons in n-$Bi_{2-x}Tl_xSe_3$ and holes in p-$Sb_{2-x}Tl_xTe_3$. The electron mobilities in n-$Bi_{2-x}Tl_xSe_3$ increase and the hole mobilities in p-$Sb_{2-x}Tl_xTe_3$ decrease upon Tl doping. In the former case, the increase in the electron mobility and the minor change in *r* suggest that the number of charged point defects decreases upon thallium doping. Thus, the decrease in the number of V^{+2}_{Se} charged point defects prevails over Tl^{-2}_{Bi} defect formation. In the case of p-$Sb_{2-x}Tl_xTe_3$, carrier scattering at charged point defects increases.

ACKNOWLEDGMENTS

This study was supported by the Russian Foundation for Basic Research (project no. IND-a 15-52-45037) and the Department of Science and Technology (DST), Government of India-RFBR (DST reference No.: INT/RUS/RFBR/P-183).

REFERENCES

1. G. S. Nolas, J. Sharp, and H. J. Goldsmid, *Thermoelectrics: Basic Principles and New Materials Developments* (Springer, New York, 2001).
2. H. J. Goldsmith, *Introduction to Thermoelectricity* (Springer,N. Y. 2010).
3. K. Behnia, *Fundamentals of Thermoelectricity* (Oxford Univ. Press, Oxford, UK, 2015).
4. G. J. Snyder and E. S. Toberer, Nature Mater. **7**, 105 (2008).
5. A. Soni, Z. Yanyuan, Y. Ligen, M. K. K. Aik, M. S. Dresselhaus, and Q. Xiong, Nano Lett. **12**, 1203 (2012).
6. A. Akrap, A. Ubaldini, E. Giannini, and L. Forro, Eur. Phys. Lett. **107**, 57008 (2014).
7. V. A. Kulbachinskii, A. Yu. Kaminsky, K. Kindo, Y. Narumi, K. Suga, S. Kawasaki, M. Sasaki, N. Miyajima, G. R. Wu, P. Lostak, and P. Hajek, Phys. Status Solidi B **229**, 1467 (2002).
8. V. A. Kulbachinskii, V. G. Kytin, P. M. Tarasov, and N. A. Yuzeeva, Phys. Solid State **52**, 1830 (2010).
9. N. B. Brandt and V. A. Kulbachinskii, Semicond. Sci. Technol. **7**, 907 (1992).
10. V. A. Kulbachinskii, Z. M. Dashevskii, M. Inoue, M. Sasaki, H. Negishi, W. S. Gao, P. Lostak, J. Horak, and A. de Visser, Phys. Rev. B **52**, 10915 (1995).
11. D. Das, K. Malik, A. K. Deb, S. Dhara, S. Bandyopadhyay, and A. Banerjee, J. Appl. Phys. **118**, 045102 (2015).
12. L. W. da Silva, M. Kaviany, and C. Uher, J. Appl. Phys. **97**, 114903 (2005).
13. S. K. Mishra, S. Satpathy, and O. J. Jepsen, J. Phys.: Condens. Matter **9**, 461 (1997).
14. A. A. Bayaz, A. Giani, A. Foucaran, F. Pascal-Delannoy, and A. Boyer, Thin Solid Films **441**, 1 (2003).
15. R. Venkatasubramanian, E. Siivola, T. Colpitts, and B. O'Quinn, Nature **413**, 597 (2001).
16. T. M. Tritt, Science **283**, 804 (1999).
17. K. Kadel, L. Kumari, W. Z. Li, J. Yu. Huang, and P. P. Provencio, Nanoscale Res. Lett. **6**, 57 (2011).
18. M. S. Dresselhaus, G. Chen, M. Y. Tang, R. Yang, H. Lee, D. Wang, Z. Ren, J. P. Fleurial, and P. Gogna, Adv. Mater. **19**, 1043 (2007).
19. P. Janíček, Č. Drašar, L. Beneš, and P. Lošt'ák, Cryst. Res. Technol. **44**, 505 (2009).
20. P. Lošt'ák, R. Novotný, J. Horák, and J. Klikorka, Phys. Status Solidi A **89**, K55 (1985).
21. A. Sher, M. Shilon, and L. Ben-dor, J. Electron. Mater. **12**, 983 (1983).
22. V. A. Kulbachinskii, A. Yu. Kaminskii, V. G. Kytin, P. Lošťák, C. Drašar, and A. de Visser, J. Exp. Theor. Phys. **90**, 1081 (2000).
23. V. A. Kulbachinskii, N. Miura, H. Nakagawa, C. Drašar, and P. Lošt'ák, J. Phys.: Condens. Matter **11**, 5273 (1999).
24. V. A. Kulbachinskii, A. A. Kudryashov, and V. G. Kytin, Semiconductors **49**, 767 (2015).
25. V. A. Kulbachinskii, A. A. Kudryashov, and V. G. Kytin, J. Phys.: Conf. Ser. **568**, 052014 (2014).
26. P. M. Koenraad, in *Delta Doping of Semiconductors*, Ed. by E. F. Schubert (Cambridge Univ. Press, Cambridge, 1996), Chap. 17
27. P. M. Koenraad, A. F. W. van de Stadt, G. Q. Hai, J. M. Shi, P. Vansant, F. Peeters, J. Devreese, J. A. A. J. Perenboom, and J. H. Wolter, Physica B **211**, 462 (1995).
28. P. T. Coleridge, R. Stoner, and R. Fletcher, Phys. Rev. B **39**, 1120 (1989).

29. V. A. Kulbachinskii, V. G. Kytin, R. A. Lunin, V. G. Mokerov, A. P. Senichkin, A. S. Bugaev, A. L. Karuzski, and A. V. Perestoronin, Semiconductors **33**, 771 (1999).

30. V. A. Kulbachinskii, L. N. Oveshnikov, R. A. Lunin, N. A. Yuzeeva, G. B. Galiev, E. A. Klimov, S. S. Pushkarev, and P. P. Maltsev, Semiconductors **49**, 921 (2015).

31. A. Isihara and L. Smrcka, J. Phys. C: Solid State Phys. **19**, 6777 (1986).

32. V. A. Kulbachinskii, R. A. Lunin, N. A. Yuzeeva, I. S. Vasilievskii, G. B. Galiev, and E. A. Klimov, Semiconductors **47**, 935 (2013).

33. V. A. Kulbachinskii, R. A. Lunin, N. A. Yuzeeva, I. S. Vasilievskii, G. B. Galiev, and E. A. Klimov, J. Exp. Theor. Phys. **116**, 755 (2013).

34. V. A. Kulbachinskii, L. N. Oveshnikov, R. A. Lunin, N. A. Yuzeeva, G. B. Galiev, E. A. Klimov, and P. P. Maltsev, Semiconductors **49**, 199 (2015).

35. E. Skuras, R. Kumar, R. L. Williams, R. A. Stradling, J. E. Dmochowski, E. A. Johnson, A. Mackinnon, J. J. Harris, R. B. Beall, C. Skierbeszewski, J. Singleton, and P. J. van der Wel, Semicond. Sci. Technol. **6**, 535 (1991).

36. V. A. Kulbachinskii, N. Miura, H. Nakagawa, H. Arimoto, T. Ikaida, P. Lošták, and C. Drašar, Phys. Rev. B **59**, 15733 (1999).

37. V. A. Kulbachinskii, N. Miura, H. Arimoto, T. Ikaida, P. Lošták, H. Horak, and C. Drašar, J. Phys. Soc. Jpn. **68**, 3328 (1999).

38. G. Offergeld and J. van Cakenberghe, J. Phys. Chem. Solids, **11**, 310 (1959).

39. A. Sklenář, C. Drašar, A. Krejčová, and P. Lošták, Cryst. Res. Technol. **35**, 1069 (2000).

Translated by A. Kazantsev